Regular Article

PHYSICAL CHEMISTRY RESEARCH
Published by the
Iranian Chemical Society
www.physchemres.org
info@physchemres.org

Phys. Chem. Res., Vol. 10, No. 2, 267-271, June 2022
DOI: 10.22036/pcr.2021.300514.1953

Structural and Morphological Studies on Strontium Tin Phosphate $SrSn(PO_4)_2$ Nanopowder

Y. Nirmal Rajeev[a,b], K. Venkatarao[a, c], B.V. Naveen Kumar[a,d], L. Bhushan Kumar[e] and S. Cole[a,*]

[a]*Dept of Physics, Acharya Nagarjuna University, Guntur 522 510, India*
[b]*Dept of Physics, V.R. Siddhartha Engineering College, Vijayawada 520 007, India*
[c]*Dept of Physics, Government Polytechnic College, Krosuru 522 410, India*
[d]*Dept of Physics, BVC College of Engineering, Rajahmundry 5333 102, India*
[e]*Dept. of Physics, SVKP Degree College, Markapur-523 316, India*

(Received 19 August 2021, Accepted 12 November 2021)

Strontium Tin phosphate $SrSn(PO_4)_2$ nanopowder was prepared by simple Solid-State Reaction method (SSR). Structural and morphological investigations of the synthesized nanopowder were characterized by Powdered X-ray diffraction study (P-XRD), Fourier transform infrared (FT-IR) Spectroscopy, Field Emission Scanning Electron Microscopy (FE-SEM), and Energy Dispersive X-ray Spectroscopy Analysis (EDS). The average crystallite size estimated from P-XRD study was around 17 nm. W-H plot method was also agreed with the size of the crystallite of the prepared sample in nanoscale. FE-SEM images show agglomerates of non-uniform biscuit like Nano flakes structure. Various functional groups of the prepared sample exhibited phosphate related bands are confirmed by FT-IR study.

Keywords: Solid-state reaction method, Nanopowder, Strontium tin phosphate

INTRODUCTION

In the 21st century, nanotechnology has been a boon to humans for materials innovation and has brought revolutionary changes in the existing technologies. In spite of new innovations for materials, controlling their structures on superfine scale and tailoring them for several applications has been achieved [1]. In recent years, phosphate-based compounds are being widely investigated due to their ease of synthesis, good homogeneity, wide band gap, high brightness, chemical/thermal stabilities over a wide range of sintering temperatures, and low cost [2]. As a host material, luminescent properties of these phosphate-based phosphor materials are of great interest. But phosphor-based families (such as nitrides, sulfates, aluminates, *etc*.) have few disadvantages besides their interesting characteristics [3].

*Corresponding author. E-mail: sandhya.cole@gmail.com

Several phosphate-based nanophosphors synthesized by various techniques have been reported [4]. The solid-state reaction method is a simple and common synthesis method to attain polycrystalline material from solid precursors in large scale usually at moderate temperatures [5]. Certain parameters such as surface area of the solids, structural properties of reactants, reactive nature and change in thermodynamical free energy are vital with the reaction [6].

Strontium (Sr) is an alkaline earth metal which plays a crucial role in bone regeneration and has several significant properties like radio-opacity and antimicrobial activity [7]. Tin phosphate phosphors are used as sorbents, electrical conductors, and catalysts [8,9]. Inorganic metal phosphates have gained special attention due to their usage in catalysis, ion exchange, luminescence, lighting, and displays [10,11]. In the present work structural and morphological studies on phosphor-based Strontium Tin phosphate nanopowder $SrSn(PO_4)_2$ synthesized by Solid-State Reaction method are reported for the first time.

Materials

Strontium Chloride hexahydrate ($SrCl_2.6H_2O$, 99.9%), Tin(IV) chloride pentahydrate ($SnCl_4.5H_2O$, 99.9%), Ammonium dihydrogen orthophosphate ($NH_4H_2PO_4$, 99.9%) and were used as starting materials for the synthesis of Strontium Tin phosphate $SrSn(PO_4)_2$ nanopowder. The chemical reaction involved in the sample preparation by Solid-State Reaction method (SSR) is given by equation as follows,

$$SrCl_2.6H_2O + 2NH_4H_2PO_4 + SnCl_4.5H_2O \longrightarrow SrSn(PO_4)_2 + 11HCl + 6H_2O + N_2 + 3H_2$$

Methodology

Strontium Tin phosphate ($SrSn(PO_4)_2$) nanopowder was synthesized by Solid-State Reaction method (SSR) with subsequent intermediate grinding and sintering at 500 °C for 2 h and 950 °C for 2 h in a programmable muffle furnace. After that, the prepared sample was allowed to cool at room temperature and is grained well. The powdered sample obtained was ultrafine. The detailed schematic preparation procedure was depicted in Fig. 1 [12].

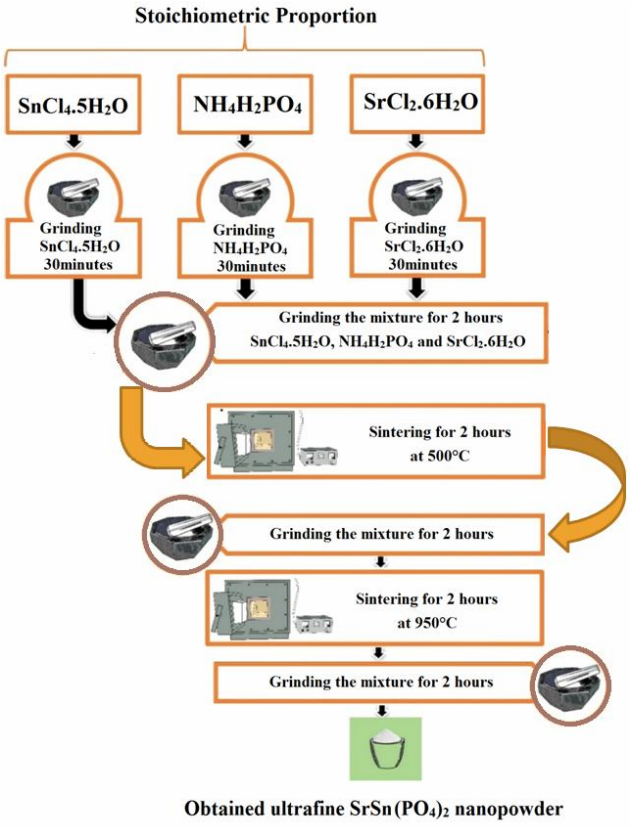

Fig. 1. Schematic preparation procedure of Strontium Tin phosphate ($SrSn(PO_4)_2$) nanopowder.

Characterizations

The Powdered X-ray diffraction pattern was recorded by Rigaku Miniflex600, Rigaku Corporation, Japan. X-ray diffractometer with Cu kα (k = 1.5406 Å), 2θ = 3° to 90° with step size 0.02° and 1.0 s time/step. Field Emission Scanning Electron Microscopy (FE-SEM) images were collected from ZEISS Sigma 300 Analytical microscope and Energy Dispersive X-ray Spectroscopy Analysis (EDS) was done using EDS: Bruker XFlash 6I30. FT-IR spectrum was recorded on Cary 630 FT-IR with Diamond attenuated total reflection (ATR), Agilent Technologies, USA Spectrometer in the range 600-4000 cm^{-1}.

RESULTS AND DISCUSSION

P-XRD Studies

Figure 2 SSR method prepared P-XRD pattern of $SrSn(PO_4)_2$ nanopowder. Sharp, broad, and well defined peaks were observed from P-XRD pattern.

Crystallite size of the prepared $SrSn(PO_4)_2$ sample was computed by Debye-Scherer's Eq. (1) also Dislocation

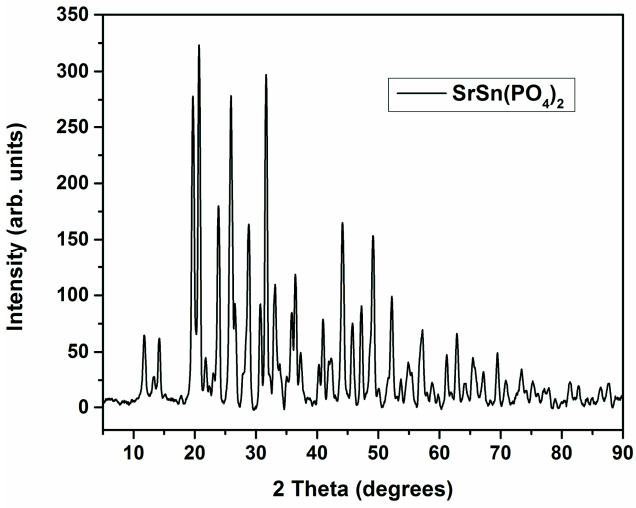

Fig. 2. P-XRD pattern of $SrSn(PO_4)_2$ nanopowder.

density (δ) (2) and micro-strain (ε) (3), respectively were evaluated using the following formulae [13].

$$D = \frac{K\lambda}{\beta \cos\theta} \quad (1)$$

$$\delta = \frac{1}{D^2} \quad (2)$$

$$\varepsilon = \frac{\beta}{4\tan\theta} \quad (3)$$

Where K is shape factor, λ is wavelength of X-rays, β is full width at half maximum (FWHM) of X-ray diffraction peaks, θ is Bragg's diffraction angle, D is average crystallite size of the lattice, δ is dislocation density and ε is microstrain.

Crystallite size (D), dislocation density (δ), and microstrain (ε) calculated from the above equations are 17 nm, 3.46×10^{15} lines/m^2, and $\varepsilon = 114.5 \times 10^{-4}$, respectively.

W-H plot Method

Williamson-Hall plot method is used to calculate the average crystallite size (D) and microstrain (ε) of the prepared nanopowder which is given by the equation

$$\beta\cos\theta = (0.9\lambda/D) + 4\varepsilon\sin\theta$$

W-H equation represents a straight line between 4sinθ on the x-axis and βcosθ on the y-axis. The y-intercept of the line represents crystallite size (D) and the slope of the line gives microstrain (ε). Figure 3 shows the W-H plot of $SrSn(PO_4)_2$ nanopowder. The values obtained from this method are D = 15 nm, δ = 4.44×10^{15} lines/m^2 and $\varepsilon = -7.548 \times 10^{-4}$.

FE-SEM and EDS Analysis

To study the topography, morphology, and distribution of particles/grains in the sample FE-SEM technique is employed. Figures 4a, b, c. shows FE-SEM micrographs of the prepared $SrSn(PO_4)_2$ nanopowder captured at 100 nm, 200 nm, and 1 μm. These images exhibit agglomerates of non-uniformly distributed biscuit like Nano-flakes. The elemental composition of the prepared nanopowder was also studied by Energy Dispersive X-ray Spectroscopy Analysis

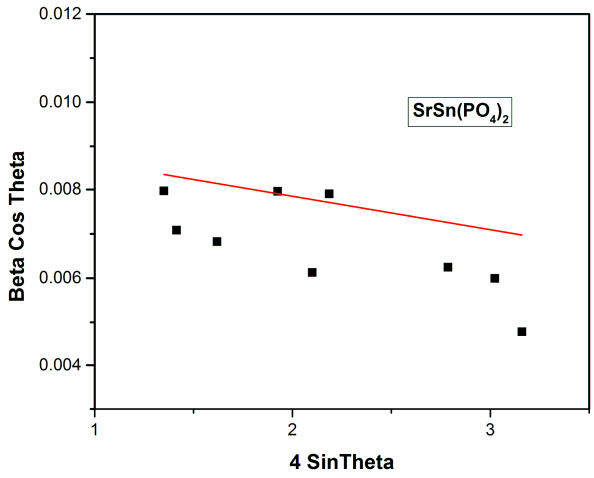

Fig. 3. W-H plot of $SrSn(PO_4)_2$ nanopowder.

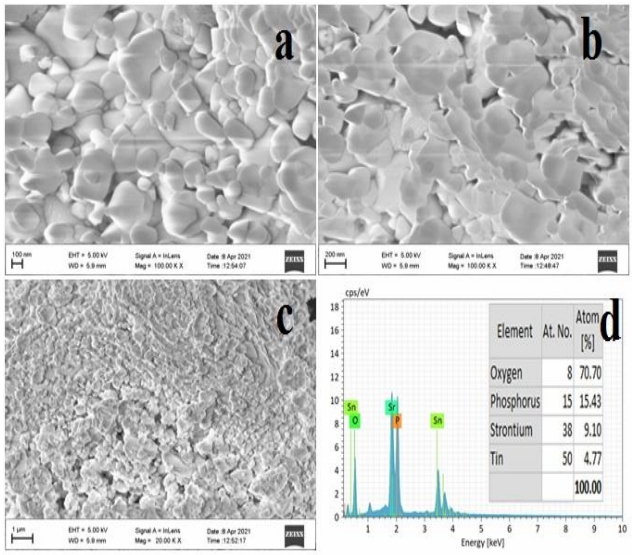

Fig. 4a, b & c. FE-SEM micrographs of the prepared $SrSn(PO_4)_2$ nanopowder captured at 100 nm, 200 nm, and 1 μm, respectively and Fig. 4d ratios and intensities of the elemental constituents present in $SrSn(PO_4)_2$ nanopowder.

(EDS). Figure 4d shows the ratios and intensities of the elemental constituents present in the SSR method prepared $SrSn(PO_4)_2$ nanopowder. The spectrum shows the presence of elements Sr, Sn, P, and O in the prepared sample and no

traces of impurities were detected. Particle/grain size distribution in the prepared sample was also obtained from ImageJ software. Figure 5a shows the mapping in the FE-SEM image and Fig. 5b shows the histogram of particle/grain size distribution of $SrSn(PO_4)_2$ nanopowder. The average particle/grain size estimated is 85.2 nm.

FT-IR study

Fundamental vibrational bands of the prepared $SrSn(PO_4)_2$ nanopowders are presented in FT-IR spectrum in the range 1500-600 cm^{-1}. Figure 6 shows the FT-IR spectrum of $SrSn(PO_4)_2$ nanopowder. It presents symmetric and asymmetric stretching and bending modes of vibration. The bands observed at 602, 612, 619, 639, and 669 cm^{-1} are attributed to asymmetric bending mode PO_4^{3-} ions (ν_4) [14]. The cluster of bands at 1007, 1043, 1077and 1184 cm^{-1}, respectively are ascribed to asymmetric stretching mode of PO_4^{3-} ions (ν_3) [15,16]. A band at 969 cm^{-1} is assigned to symmetric stretching mode of PO_4^{3-} ions (ν_1) [12]. An infrared band observed at 746 cm^{-1} is attributed to symmetric stretching mode of P-O-P bridge [1]. A band observed at 1234 cm^{-1} is assigned to PO_2^- vibrations. The existence of phosphate group ions in the madden sample was confirmed from the spectrum. The identified band positions and assignments are given in Table 1.

CONCLUSIONS

$SrSn(PO_4)_2$ nanopowder was successfully prepared by Solid-State Reaction method (SSR). The average crystallite size calculated by Debye Scherer's formula was around 17 nm and that of the W-H plot method was around 15 nm. FE-SEM micrographs show agglomerates of non-uniformly distributed biscuit like flakes of the prepared samples. EDS confirmed all the desired elements in the sample without any traces of impurities. FT-IR study indicates the presence of vibrational modes of phosphate ions.

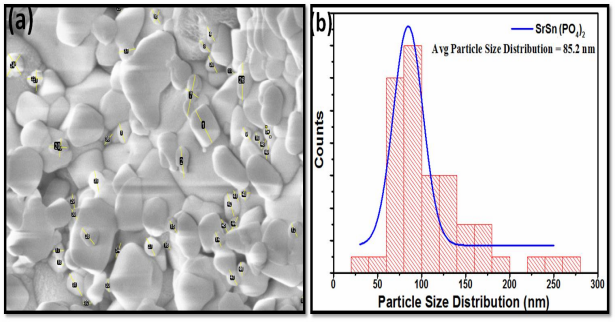

Fig. 5a. Mapping in the FE-SEM image and **Fig. 5b.** Histogram of particle/grain size distribution of $SrSn(PO_4)_2$ nanopowder.

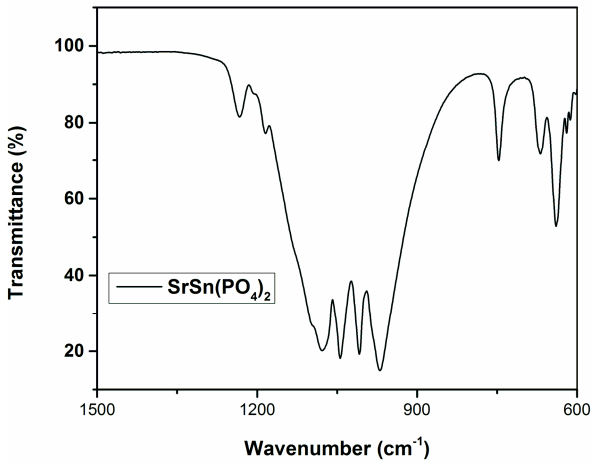

Fig. 6. FT-IR spectrum of $SrSn(PO_4)_2$ nanopowder.

Table 1. FT-IR Vibrational Band Assignments of $SrSn(PO_4)_2$ Nanopowder

S. No.	Band position (cm^{-1})	Characteristic feature
1	602, 612, 619, 639 and 669	asymmetric bending mode PO_4^{3-} ions (ν_4)
2	1007, 1043, 1077 and 1184	asymmetric stretching mode of PO_4^{3-} ions
3	969	symmetric stretching mode of PO_4^{3-} ions (ν_1)
4	746	symmetric stretching mode of P-O-P bridge
5	1234	PO_2^- vibrations

Conflicts of Interest

The authors declare no conflict of interest.

REFERENCES

[1] Munimasthani, S.; Sarathkumar, S.; Khidhirbrahmendra, V., Ravikumar, R.V.S.S.N. Structural studies of Nd^{3+} doped cadmium calcium pyrophosphate nanophosphors. *Mater. Today: Proc.* **2020**, *26*, 114-116, https://doi.org/10.1016/j.matpr.2019.05.445.

[2] Wani, J. A.; Dhoble, N. S.; Kokode, N. S.; Singh, V.; Dhoble, S. J., Dy^{3+} -, Sm^{3+} -, Ce^{3+} - and Tb^{3+}- activated optical properties of microcrystalline $BaMgP_2O_7$ phosphors. *Luminescence* **2017**, *32*, 240-252, https://doi.org/10.1002/bio.3176.

[3] Deng, D.; Yu, H.; Li, Y.; Hua, Y.; Jia, G.; Zhao, S.; Wang, H.; Huang, L.; Li, Y.; Li, C. *et al.* $Ca_4(PO_4)_2O$: Eu^{2+} red-emitting phosphor for solid-state lighting: structure, luminescent properties and white light emitting diode application. *J. Mater. Chem.* **2013**, *1*, https://doi.org/10.1039/c3tc30148f.

[4] Chander, H., Development of nanophosphors-A review. *Mater. Sci. Eng. R Rep.* **2005**, *49*, 113-155, https://doi.org/10.1016/j.mser.2005.06.001.

[5] West, A. R., Solid State Chemistry and its Applications: John Wiley & Sons, **2014**.

[6] Tucureanu, V.; Matei, A.; Avram, A. M., Synthesis and characterization of YAG: Ce phosphors for white LEDs. Opto-Electron. Rev. **2015**, *23*, 239-251, DOI: https://doi.org/10.1515/oere-2015-0038.

[7] Zhou, H.; Nedley, M.; Bhaduri, S. B., The impacts of Mg^{2+} on strontium phosphate: A preliminary study. *Mater. Lett.* **2013**, *113*, 63-66, https://doi.org/10.1016/j.matlet.2013.09.079.

[8] Mal, N. K.; Ichikawa, S.; Fujiwara, M., Synthesis of a novel mesoporous tin phosphate, $SnPO_4$. *Chem. Commun. (Camb.)* **2002**, *1*, 112-113, https://doi.org/10.1039/b109948e.

[9] Rao, K. T. V.; Souzanchi, S.; Yuan, Z.; Ray, M. B.; Xu, C., Simple and green route for preparation of tin phosphate catalysts by solid-state grinding for dehydration of glucose to 5-hydroxymethylfurfural (HMF). *RSC Adv.* **2017**, *7*, 48501-48511, https://doi.org/10.1039/c7ra10083c.

[10] Hussin, R.; Hamdan, S.; Halim, D. N. F. A.; Husin, M. S., The origin of emission in strontium magnesium pyrophosphate doped with Dy_2O_3. *Mater. Chem. Phys.* **2010**, *121*, 37-41, https://doi.org/10.1016/j.matchemphys.2009.12.033.

[11] Yang, Y.; Qiu, Y.; Gong, P.; Kang, L.; Song, G.; Liu, X.; Sun, J.; Lin, Z., Lone-pair enhanced birefringence in an alkaline-earth metal tin(II) phosphate $BaSn_2(PO_4)_2$. *Chemistry* **2019**, *25*, 5648-5651, https://doi.org/10.1002/chem.201806108.

[12] Sarathkumar, S.; Munimasthani, S.; Thampy, U. S. U.; Ravikumar, R. V. S. S. N., Structural and luminescent properties of $CaZn_2(PO_4)_2$: RE^{3+} (RE = Er and Pr) nanophosphors for versatile device applications. *J. Mater. Sci. Mater. Electron.* **2020**, *31*, 11589-11598, https://doi.org/10.1007/s10854-020-03707-x.

[13] Sreedevi, G.; Muswareen, S. K. K.; Jayalakshmi, V.; Cole, S., Effect of TiO_2 doping on structural and optical properties of $CdSZn_3(PO_4)_2$ nanocomposites. *Appl. Phys. A* **2019**, *125*, 1-11, https://doi.org/10.1007/s00339-019-3037-3.

[14] Pawlig, O.; Trettin, R., Synthesis and characterization of α-hopeite, $Zn_3(PO_4)_2 \cdot 4H_2O$. *Mater. Res. Bull.* **1999**, *34*, 1959-1966, DOI: https://doi.org/10.1016/S0025-5408(99)00206-8.

[15] Frost, R. L.; Scholz, R.; Lopez, A.; Xi, Y., A vibrational spectroscopic study of the phosphate mineral whiteite $CaMn^{(++)}Mg_2Al_2(PO_4)_4(OH)_{2.8}(H_2O)$. *Spectrochim. Acta A Mol. Biomol. Spectrosc.* **2014**, *124*, 243-248, https://doi.org/10.1016/j.saa.2014.01.053.

[16] Balan, E.; Delattre, S.; Roche, D.; Segalen, L.; Morin, G.; Guillaumet, M.; Blanchard, M.; Lazzeri, M.; Brouder, C.; Salje, E. K. H., Line-broadening effects in the powder infrared spectrum of apatite. *Phys. Chem. Miner.* **2010**, *38*, 111-122, https://doi.org/10.1007/s00269-010-0388-x.